

Collinear two-photon state with spectral properties of type-I and polarization properties of type-II spontaneous parametric down-conversion: Preparation and testing

A. V. Burlakov, M. V. Chekhova, O. A. Karabutova, and S. P. Kulik

Department of Physics, Moscow State University, 119899 Moscow, Russia

(Received 28 February 2001; published 17 September 2001)

Two beams of collinear type-I biphotons generated via spontaneous parametric down-conversion (SPDC) from coherent pump beams are transformed without a loss into a state of correlated photons with orthogonal (in the general case, elliptical) polarizations. This alternative state manifests remarkable properties: while having the spectrum of type-I SPDC, it has polarization properties similar to type-II SPDC. To test the state, we use the anticorrelation effect (“anticorrelation dip”).

DOI: 10.1103/PhysRevA.64.041803

PACS number(s): 42.50.Dv, 03.67.—a

Spontaneous parametric down-conversion (SPDC) [1] is at present the simplest way of generating entangled, or non-factorizable states of two photons. This effect can be briefly described as a spontaneous decay of pump photons into pairs of correlated photons (called signal and idler) in a material with quadratic nonlinearity. Such pairs of correlated photons are called biphotons [2]. Polarization of signal and idler photons can be either the same or orthogonal; in the first case, the process is called type-I SPDC, in the second one, type-II SPDC. Depending on the particular type of phase matching, the signal and idler photons can also differ by frequency and wave-vector direction [1]. For example, in the case of frequency-degenerate collinear type-I phase matching, they belong to the same mode of radiation and can be considered as indistinguishable. When used in this regime, SPDC produces a two-photon Fock state $|2\rangle$ [3], naturally, as a small addition to the vacuum state. The state generated in frequency-degenerate collinear type-II SPDC is a two-mode state, since it involves two polarization modes; in the two-mode notation, it can be written as $|1,1\rangle$.

One of the most elegant effects revealing the nonclassical properties of biphoton fields is the so-called anticorrelation effect [4]. The effect is observed by sending signal and idler photons to the input ports of a 50% beam splitter. After the beam splitter, two detectors are registering radiation in the two output modes, and their coincidences are analyzed. The dependence of the coincidence counting rate on the delay between signal and idler photons before the beam splitter has a typical “dip” shape. When the path lengths of signal and idler photons before the beam splitter are perfectly equal, which means that an observer registering a coincidence cannot tell whether it was caused by two transmitted photons or two reflected photons, the rate of coincidence counting drops down to the level of accidental coincidences. The shape of the anticorrelation dip is different for type-I and type-II SPDC. It has been shown [4–6] that the dip shape reflects the first-order correlation function for SPDC radiation, which, in its turn, is the Fourier transform of the spectrum. For frequency-degenerate type-I SPDC, the spectrum is broader [7], which leads to a narrow anticorrelation dip. This fact was used in the works on measuring small group delays between signal and idler photons [8]. Observation of the anticorrelation effect for collinear type-II SPDC has an important advantage: the delay between signal and idler photons is

introduced by means of a birefringent material [9]. The resulting polarization interferometer is much more stable than a spatial one used for observing anticorrelation effect with type-I SPDC.

Recently, it has been suggested to prepare type-II collinear biphoton radiation from type-I collinear SPDC [10]. Preparation is essentially based on two-photon interference, namely, on the fact that two different nonlinear crystals pumped by the same laser beam emit photon pairs coherently. One can observe interference between coincidences caused by pairs born in different crystals. Consider now two crystals of equal length both generating type-I SPDC from the same pump (or coherent pump beams with equal intensities); if polarization of biphotons (signal and idler photons) from the first crystal is orthogonal to the polarization of biphotons from the second one, the state at the output can be represented as a superposition [11]

$$\psi = \frac{1}{\sqrt{2}}(|2,0\rangle + e^{i\epsilon}|0,2\rangle), \quad (1)$$

where $|n,m\rangle$ is a two-photon ($n+m=2$) two-mode state with n photons polarized horizontally and m photons polarized vertically [12,13]. A similar two-crystal scheme has been recently suggested for noncollinear nonmaximally polarization-entangled states preparation [14], used for testing Bell’s inequalities [15], and applied for preparing collinear two-color Bell states [16]. The phase ϵ can be varied in different ways (see the experiment below). One can show that Eq. (1) can be represented as a two-photon state

$$\psi = |1,1\rangle_{\epsilon} \equiv a_{\epsilon}^{\dagger} a_{\epsilon\perp}^{\dagger} |0,0\rangle, \quad (2)$$

where a_{ϵ}^{\dagger} is the operator of photon creation in the mode corresponding to right elliptical polarization with the axes of the ellipse oriented at $\pm 45^{\circ}$ to the vertical axis. It can be represented in the linear polarization basis as $a_{\epsilon}^{\dagger} = 1/\sqrt{2}(a_x^{\dagger} + ie^{i\epsilon/2}a_y^{\dagger})$. Similarly, the operator $a_{\epsilon\perp}^{\dagger} = 1/\sqrt{2}(a_x^{\dagger} - ie^{i\epsilon/2}a_y^{\dagger})$ corresponds to orthogonally polarized light. The phase ϵ determines the ellipticity of the polarization modes. In particular, for $\epsilon=0$ we obtain the state of correlated right- and left-polarized photons, $|1,1\rangle_{\pm}$, and for $\epsilon=\pi$ the state is $|1,1\rangle_{\pm 45^{\circ}}$, a pair of correlated photons polarized linearly at $\pm 45^{\circ}$ to vertical axis. In other words, the synthesized state is similar to the state generated via type-II SPDC $|1,1\rangle$ and can be transformed into it by using an appropriate retardation

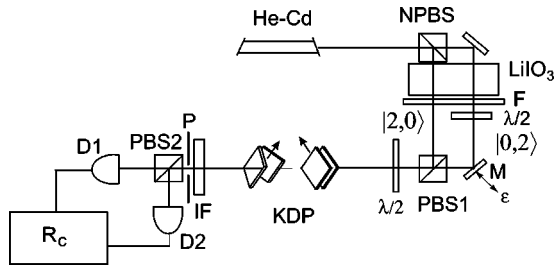


FIG. 1. The experimental setup. Preparation part: SPDC is coherently excited in two spatial domains of the LiIO_3 crystal. NPBS is a nonpolarizing beam splitter, F a pump-cutting filter, PBS1 a polarizing beam splitter, M a mirror scanned for varying phase ϵ . Registration part: an interference filter IF, a pinhole P, a polarizing beam splitter PBS2, detectors D1, D2, the coincidence circuit. Four KDP plates, oriented at $\pm 45^\circ$ to Y, serve for delay variation.

plate. Similar transformations using the state $|1,1\rangle_{\pm 45^\circ}$ as a starting point have been reported in [17]. Since linear optical elements used for preparing the state (2) do not change its spectral properties, the synthesized state (2) should have the spectrum corresponding to type-I frequency-degenerate phase matching,

$$S(\omega) = \frac{\sin^2(L(\omega - \omega_0)^2/2s)}{(L(\omega - \omega_0)^2/2s)^2}, \quad (3)$$

where ω_0 is the central frequency of SPDC spectrum in the degenerate case, equal to half of the pump frequency ω_p , L is the crystal thickness, and s is inverse to the second derivative of the crystal dispersion dependence $k(\omega)$, $s \equiv (d^2k/d\omega^2)^{-1}$. Having the spectral properties of “type-I” SPDC radiation, the synthesized state (2) should at the same time have polarization properties similar to type-II SPDC radiation. For instance, it should manifest hidden polarization [18]. The anticorrelation effect for this state can be observed by introducing polarization delay between signal and idler photons. In the particular case $\epsilon = \pi$, this is done by inserting birefringent material with the optic axis oriented at 45° to the vertical axis.

In our experiment (Fig. 1), collinear frequency-degenerate type-I SPDC is obtained in a 15-mm lithium iodate crystal from a cw He-Cd laser with a wavelength of 325 nm. The crystal is placed into a Mach-Zehnder interferometer, so that two SPDC beams are coherently generated in separate domains. A half-wave plate is inserted into one of the beams, rotating the polarization by 90° , and the two SPDC beams are joined using a polarizing beam splitter PBS1. The state at the output is given by Eq. (1) and can be also written in the form (2). The phase ϵ can be varied by scanning mirror M of the Mach-Zehnder interferometer. At $\epsilon = \pi$, the state (2) is a type-II biphoton in the basis rotated by 45° . A half-wave plate oriented at 22.5° to the vertical axis converts it into the state $|1,1\rangle$ in the XY basis. Preparation of this state is tested by means of a polarizing beam splitter PBS2, a pair of avalanche diodes, and a coincidence circuit with resolution 1.5 ns. For spatial and spectral selection, a pinhole P and an interference filter IF are inserted into the beam. We use two

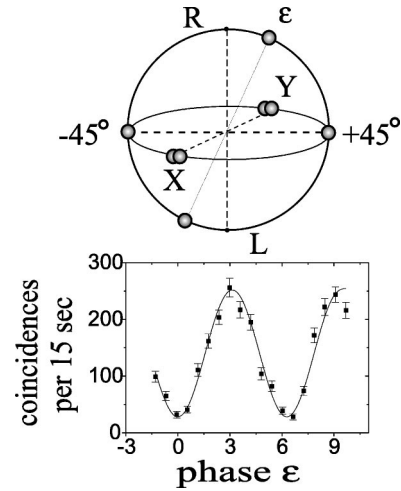


FIG. 2. Top: different collinear biphoton states shown on the Poincaré sphere. The initial states, $|2,0\rangle$ and $|0,2\rangle$, are polarized, respectively, along X and Y; the produced state $|1,1\rangle_\epsilon$ is shown as a pair of dots placed oppositely on the same meridian, but with the latitude depending on ϵ . For $\epsilon = \pi$, the state is $|1,1\rangle_{\pm 45^\circ}$. Bottom: dependence of the coincidence counting rate on ϵ . $\lambda/2$ plate after the interferometer is put at 22.5° , so that for $\epsilon = \pi, 3\pi, \dots$ the state after the plate is $|1,1\rangle$.

kinds of interference filters, both centered at wavelength 650 nm: with bandwidth 10 nm and with bandwidth 40 nm. In the last case, the filter does not restrict the SPDC spectrum (which has width 18 nm) and serves only for noise suppression.

Figure 2 demonstrates possible collinear two-photon states generated via SPDC. Polarization is shown on the Poincaré sphere where the equator represents states with linear polarization, the poles correspond to right and left circular polarization, and the opposite points depict orthogonally polarized light. The states $|2,0\rangle$ and $|0,2\rangle$ generated via type-I SPDC are shown as “double dots” polarized along X and Y, respectively. The state generated via type-II SPDC (not shown in the figure) would correspond to a pair of opposite dots, placed at X and Y positions. The state $|1,1\rangle_\epsilon$, which we generate experimentally, is a pair of opposite dots corresponding to the same longitude, but varying latitude. At $\epsilon = \pi$, the state is a pair of photons polarized linearly at $\pm 45^\circ$. Testing of this state is shown on the bottom of Fig. 2: coincidence counting rate is plotted versus the phase ϵ (mirror M position). The half-wave plate after the interferometer (Fig. 1) is oriented at 22.5° . The filter bandwidth is 40 nm. At certain positions of the mirror, corresponding to $\epsilon = \pi$, a maximum of the coincidence counting rate is observed, which indicates that the state $|1,1\rangle$ is created after the plate. (Before the plate, the state is $|1,1\rangle_{\pm 45^\circ}$.) Note that in an ideal case, the transformation is complete [10] and the visibility of the pattern equals 100%. The dependence in Fig. 2 has 85% visibility, which can be explained by nonequal losses in the arms of the interferometer and slight misalignment.

To measure the anticorrelation dip, we fix the phase $\epsilon = \pi$, which gives us the state $|1,1\rangle_{\pm 45^\circ}$, and put the half-wave plate after the interferometer in the 0° position [19]. A variable delay τ between the correlated photons is introduced

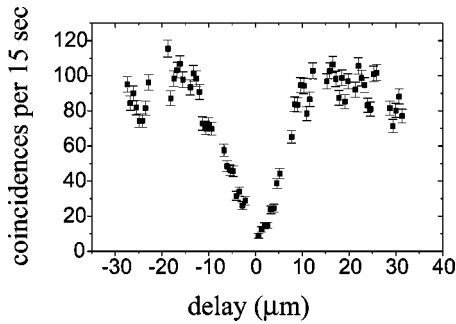


FIG. 3. The anticorrelation “dip” observed with a 40-nm filter.

by means of two pairs of KDP crystals with thickness 1.17 mm. The optic axes for one pair are oriented at $+45^\circ$, for the other pair at -45° (Fig. 1). To vary the delay, one pair of crystals is tilted in the opposite direction around the optic axes. For untilted plates, the total delay is zero due to the orthogonal orientation of optic axes for the two pairs of plates. For additional delay variation, quartz plates are used. After the delay, the biphoton beam is directed to polarizing beam splitter PBS2, whose output modes correspond to X and Y polarizations. Hence, PBS2 acts for the input state as a 50% nonpolarizing beam splitter, and the coincidence counting rate should show the anticorrelation dip. This is shown in Fig. 3, where the coincidence counting rate is plotted against the delay τ . It should be mentioned that complete transformation of type-I biphotons into type-II biphotons occurs only for a perfectly adjusted interferometer, with the phase ϵ exactly equal to π . In this ideal case, the counting rates of the detectors do not depend on τ (there is no first-order interference). The drift of the phase and other instabilities lead to a modulation in both single-counting rates and the coincidence counting rate. For a better analysis of the dip shape, we measure its right-hand part with a more careful adjustment of the phase at each point. To compare the dip shape with the correlation function $g^{(1)}(\tau)$ of type-I SPDC, we also measure $g^{(1)}(\tau)$ as follows. One arm of the interferometer is closed, so that the state after PBS1 is of the form $|2,0\rangle$, i.e., it is horizontally polarized. The KDP and quartz crystals split this beam and introduce the delay τ between the field components polarized at $\pm 45^\circ$. Finally, PBS2 projects both field components onto XY directions. The intensities measured by the detectors $D_{1,2}$ show antiphased modulation, $I_{1,2} \sim 1 \pm V(\tau)\cos(\omega_0\tau)$, with the visibility equal to the modulo of the first-order correlation function, $V = |g^{(1)}(\tau)|$. The interference visibility as a function of the delay τ is plotted in Fig. 4(a) and the corresponding dip shape in Fig. 4(b). Note that both curves in Figs. 4(a) and 4(b) are obtained in the same experimental run and therefore correspond to the same orientation of the nonlinear crystal. This is very important since the spectrum of type-I SPDC, and hence the dip shape, strongly depend on the crystal orientation. The fitting curve in Fig. 4(a) is calculated by taking the Fourier transform of the type-I SPDC spectrum (3).

Theoretical consideration gives a simple expression for the dip shape: for an arbitrary shape of the SPDC spectrum $S(\Omega)$, $\Omega \equiv \omega - \omega_0$, the coincidence counting rate depends on τ as

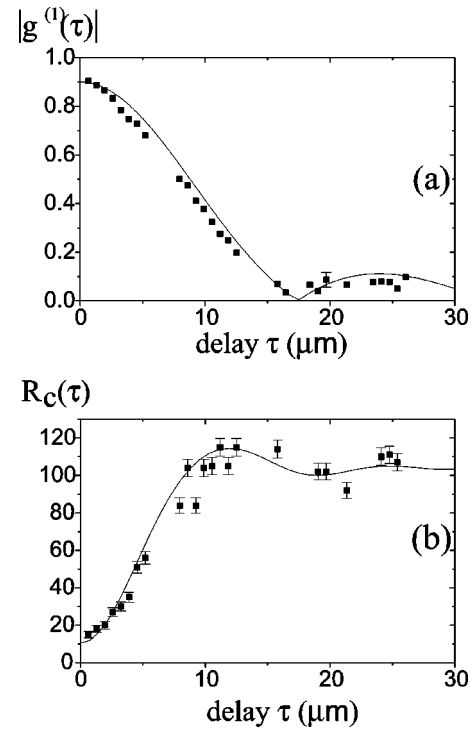


FIG. 4. The first-order correlation function absolute value (a) and the “dip” shape (b) for the case of the 40-nm filter.

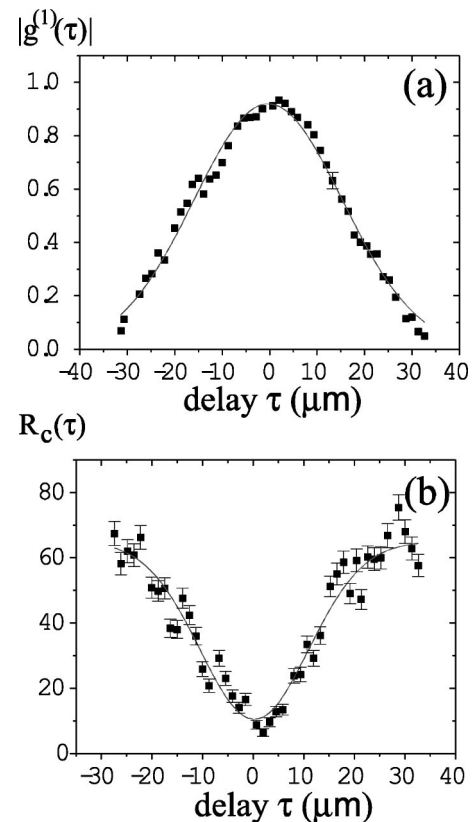


FIG. 5. The first-order correlation function (a) and the anticorrelation “dip” (b) for the case of the 10-nm filter.

$$R_c \sim 1 - g^{(1)}(2\tau), g^{(1)}(\tau) = \frac{1}{2\pi} \int S(\Omega) \cos \Omega \tau d\Omega, \quad (4)$$

i.e., the dip width is exactly twice smaller than $g^{(1)}(\tau)$ width. This expression agrees with the results of [4–6,9]; for instance, in the type-II case [9], both $g^{(1)}(\tau)$ and the dip have a triangular shape, but the base of the dip is DL , with D denoting the inverse group velocity difference between signal and idler photons, while the base of $g^{(1)}(\tau)$ is twice as large. In accordance with relation (4), the dip shape in Fig. 4(b) corresponds well to the twice squeezed and inverted $g^{(1)}$ shape. Note that relation (4) is valid only for the case of the unfiltered SPDC. If Gaussian filters are used in both signal and idler channels, the result is different. Since the dip shape is a fourth-order function of the field, while the first-order correlation function is quadratic in the field, spectral filtering has a different effect on their shape. Calculation shows that for a Gaussian filter with width given by parameter σ , the dip shape should take the form

$$R_c \sim 1 - \frac{1}{2\pi} \int e^{-(\Omega)^2/4\sigma^2} \cos \Omega \tau d\Omega, \quad (5)$$

which is $\sqrt{2}$ narrower than the corresponding correlation function $g^{(1)}(\tau)$. This fact is demonstrated experimentally in Figs. 5(a) and 5(b), where R_c and $g^{(1)}$ are plotted versus τ

for the case of 10-nm filter inserted into the SPDC beam. The fitting Gaussian curves differ in width by 1.46, which is close to $\sqrt{2}$.

To conclude, in our experiment we prepared and tested a special two-photon state whose spectral properties are the same as for type-I SPDC, but polarization properties resemble those of type-II SPDC. The anticorrelation effect for this state can be observed with a polarization interferometer, as for type-II, and gives a very narrow dip, as for type-I. For the 15-mm LiIO₃ crystal and broad-band filter, the dip width is 30 fs; using a 1-mm crystal would give a dip with width 8 fs. Hence, the synthesized state can be used for precise measurement of group delays between orthogonally polarized photons. Moreover, the set of states available with our preparation technique includes elliptically polarized signal-idler pairs; this suggests a possibility for accurate measurement of group delays between elliptically polarized photons. Note that the experiment is carried out in collinear geometry, which is convenient for quantum communication.

We would like to thank G.O. Rytikov for considerable help in the experiment. This work was supported in part by the Russian Foundation for Basic Research, Grant Nos. 99-02-16419 and 00-15-96541. We also acknowledge support of the Russian Federation Integration Program “Basic Optics and Spectroscopy.”

-
- [1] D.N. Klyshko, *Photons and Nonlinear Optics* (Gordon & Breach, New York, 1988).
- [2] D.N. Klyshko, Zh. Éksp. Teor. Fiz **83**, 1313 (1982) [Sov. Phys. JETP **56**, 755 (1982)].
- [3] See, for instance, M.O. Scully and M.S. Zubairy, *Quantum Optics* (Cambridge University Press, Cambridge, 1997).
- [4] C.K. Hong, Z.Y. Ou, and L. Mandel, Phys. Rev. Lett. **59**, 2044 (1987).
- [5] J.G. Rarity and P.R. Tapster, JOSA B **6**, 1221 (1989).
- [6] A.V. Belinsky and D.N. Klyshko, Laser Phys. **4**, 663 (1994).
- [7] A.V. Burlakov, M.V. Chekhova, D.N. Klyshko, S.P. Kulik, A.N. Penin, Y.H. Shih, and D.V. Strekalov, Phys. Rev. A **56**, 3214 (1997).
- [8] A.M. Steinberg, P.G. Kwiat, and R.Y. Chiao, Phys. Rev. Lett. **68**, 2421 (1992).
- [9] Y.H. Shih and A.V. Sergienko, Phys. Lett. A **186**, 29 (1994); *ibid.* **191**, 201 (1994).
- [10] A.V. Burlakov, M.V. Chekhova, O.A. Karabutova, D.N. Klyshko, and S.P. Kulik, Phys. Rev. A **60**, R4209 (1999).
- [11] Actually, the state also includes the vacuum contribution, but it has no effect in our experiment.
- [12] A.V. Burlakov and D.N. Klyshko, Pisma Zh. Éksp. Teor. Fiz. **69**, 795 (1999) [JETP Lett. **69**, 839 (1999)].
- [13] D.N. Klyshko, Zh. Éksp. Teor. Fiz. **111**, 1955 (1997) [JETP **84**, 1065 (1996)].
- [14] P.G. Kwiat, E. Waks, A.G. White, I. Appelbaum, and P. Eberhard, Phys. Rev. A **60**, R773 (1999).
- [15] G. Brida, M. Genovese, C. Novero, and E. Predazzi, Phys. Lett. A **286**, 12 (2000).
- [16] Y.H. Kim, S.P. Kulik, and Y.H. Shih, Phys. Rev. A **63**, 060301(R) (2001).
- [17] T. Tsegaye, J. Söderholm, M. Atatüre, A. Trifonov, G. Björk, A.V. Sergienko, B.E.A. Saleh, and M.C. Teich, Phys. Rev. Lett. **85**, 5013 (2000).
- [18] D.N. Klyshko, Phys. Lett. A **163**, 349 (1992).
- [19] The same effect is achieved by removing the plate.